

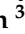



Article

1,4-Naphthoquinone Motif in the Synthesis of New Thiopyrano[2,3-*d*]thiazoles as Potential Biologically Active Compounds

Andrii Lozynskiy ¹, Julia Senkiv ², Iryna Ivasechko ², Nataliya Finiuk ² , Olga Klyuchivska ² , Nataliya Kashchak ², Danylo Lesyk ¹, Andriy Karkhut ³, Svyatoslav Polovkovych ³ , Oksana Levytska ⁴, Olexandr Karpenko ⁵, Assyl Boshkayeva ⁶, Galiya Sayakova ⁶, Andrzej Gzella ⁷, Rostyslav Stoika ² and Roman Lesyk ^{1,8,*} 

¹ Department of Pharmaceutical, Organic and Bioorganic Chemistry, Danylo Halytsky Lviv National Medical University, Pekarska 69, 79010 Lviv, Ukraine

² Institute of Cell Biology of National Academy of Sciences of Ukraine, Drahomanov14/16, 79005 Lviv, Ukraine

³ Department of Technology of Biologically Active Substances, Pharmacy and Biotechnology, Lviv Polytechnic National University, Bandera 12, 79013 Lviv, Ukraine

⁴ Department of Organization and Economics of Pharmacy, Danylo Halytsky Lviv National Medical University, Pekarska 69, 79010 Lviv, Ukraine

⁵ Enamine Ltd., 23 Alexandra Matrosova, 01103 Kyiv, Ukraine

⁶ Department of Pharmaceutical and Toxicological Chemistry, Pharmacognosy and Botany, Asfendiyarov Kazakh National Medical University, Almaty 050000, Kazakhstan

⁷ Department of Organic Chemistry, Poznan University of Medical Sciences, Grunwaldzka 6, 60-780 Poznan, Poland

⁸ Department of Biotechnology and Cell Biology, Medical College, University of Information Technology and Management in Rzeszow, Sucharskiego 2, 35-225 Rzeszow, Poland

* Correspondence: dr_r_lesyk@org.lviv.net; Tel.: +380-677-038-010



Citation: Lozynskiy, A.; Senkiv, J.; Ivasechko, I.; Finiuk, N.; Klyuchivska, O.; Kashchak, N.; Lesyk, D.; Karkhut, A.; Polovkovych, S.; Levytska, O.; et al. 1,4-Naphthoquinone Motif in the Synthesis of New Thiopyrano [2,3-*d*]thiazoles as Potential Biologically Active Compounds. *Molecules* **2022**, *27*, 7575. <https://doi.org/10.3390/molecules27217575>

Academic Editors: Carla Boga and Gabriele Micheletti

Received: 17 October 2022

Accepted: 2 November 2022

Published: 4 November 2022

Publisher's Note: MDPI stays neutral with regard to jurisdictional claims in published maps and institutional affiliations.



Copyright: © 2022 by the authors. Licensee MDPI, Basel, Switzerland. This article is an open access article distributed under the terms and conditions of the Creative Commons Attribution (CC BY) license (<https://creativecommons.org/licenses/by/4.0/>).

Abstract: A series of 11-substituted 3,5,10,11-tetrahydro-2*H*-benzo[6,7]thiochromeno[2,3-*d*][1,3]thiazole-2,5,10-triones were obtained via *hetero*-Diels-Alder reaction of 5-alkyl/arylallylidene/-4-thioxo-2-thiazolidinones and 1,4-naphthoquinones. The structures of newly synthesized compounds were established by spectral data and a single-crystal X-ray diffraction analysis. According to U.S. NCI protocols, compounds **3.5** and **3.6** were screened for their anticancer activity; 11-Phenethyl-3,11-dihydro-2*H*-benzo[6,7]thiochromeno[2,3-*d*]thiazole-2,5,10-trione (**3.6**) showed pronounced cytotoxic effect on leukemia (Jurkat, THP-1), epidermoid (KB3-1, KBC-1), and colon (HCT116wt, HCT116 p53-/-) cell lines. The cytotoxic action of **3.6** on p53-deficient colon carcinoma cells was two times weaker than on HCT116wt, and it may be an interesting feature of the mechanism action.

Keywords: 1,4-naphthoquinones; *hetero*-Diels-Alder reaction; thiopyrano[2,3-*d*]thiazoles; X-ray; anticancer activity; cytotoxicity; DNA intercalation

1. Introduction

1,4-Naphthoquinones are a large group of biologically active molecules found in various higher plants (plant families *Juglandaceae*, *Plumbaginaceae*, *Boraginaceae*, *Ebenaceae*, *Droseraceae*, *Lythraceae*, *Rubiaceae*, *Balsaminaceae*, *Bignoniaceae*, and *Ulmaceae*), lichens, bacteria, and invertebrates (especially in arthropods and echinoderms) [1]. In natural sources, 1,4-naphthoquinones often exist in a reduced form or as glycosides [2]. Some drugs, products used in cosmetology, and biologically active additives contain naphthoquinone derivatives as an active component. In particular, vitamin K₁ and menadione, as their synthetic analogs, are well-known drugs used as hemostatic agents, causing an increase in the synthesis of prothrombin and proconvertin [3,4]. Atovaquone is a synthetic antiprotozoal agent for the prevention and treatment of *Pneumocystis jirovecii* pneumonia (PCP) and malaria [5,6]. Menatetrenone is a form of vitamin K₂ for the treatment of osteoporosis

to stimulate osteogenesis. Currently, several 1,4-naphthoquinones (i.e., phyloquinone for regulation of blood coagulation, bone metabolism, and vascular biology), lawsone (natural dye), naphthazarin (natural dye), and atovaquone (antineumococcal), are used both parenterally and externally [7].

In general, 1,4-naphthoquinone derivatives, similarly to other quinones, manifest their pharmacological potential via two mechanisms [1]. The first is related to the redox properties of naphthoquinones, which are easily reduced and re-oxidized under physiological conditions. Thus, naphthoquinone derivatives in the presence of molecular oxygen and appropriate reducing agents catalyze the transfer of electrons from NADPH or thiols, which leads to the generation of various reactive oxygen species (ROS); in particular, superoxide anion, hydroxyl radicals, and hydrogen peroxide [8,9]. The second mechanism is based on the high electrophilicity of 1,4-naphthoquinone derivatives. This property allows 1,4-naphthoquinones to form covalent bonds with nucleophilic agents and interact with thiol groups of proteins, glutathione, and nucleophilic amino acid groups; for example, with the terminal amino group of lysine [1]. Accordingly, this complex of properties made it possible to identify several highly active anticancer [10–12], antibacterial [13], antifungal [14], anti-inflammatory [15,16], and antiparasitic agents [17–20] (Figure 1). Furthermore, some 1,4-naphthoquinone derivatives were found as efficient inhibitors of proteasomes [21], N-acetyltransferase [11], cyclin-cyclin-dependent kinase [22], aldose reductase [16], topoisomerases I and II [23,24], heat shock proteins [25], DNA gyrase [26], phosphatidylinositol 3-kinase [27], and inhibitors of Stat3 [28] and cancer stem cell cascades [11].

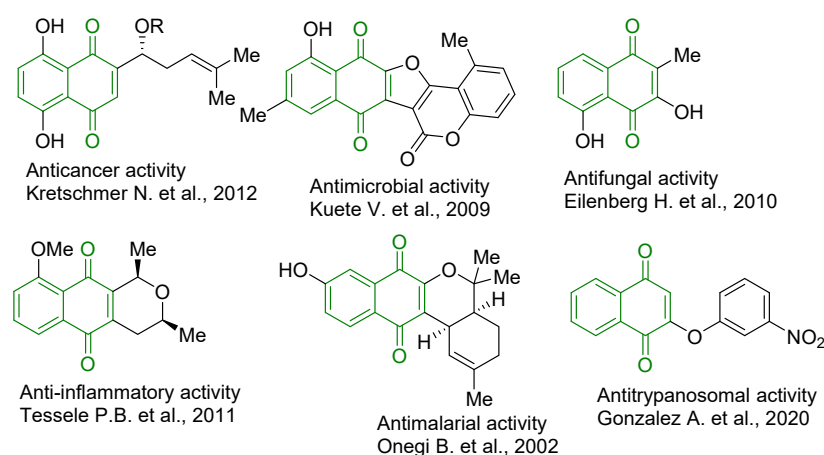


Figure 1. Structures of biologically active 1,4-naphthoquinone derivatives [12–15,17,19].

Additionally, 1,4-naphthoquinone derivatives are an interesting scaffold for various types of chemical transformations. Thus, being active dienophiles, they undergo Diels–Alder reactions, which are often accompanied by variability in regio- and diastereoselectivity processes depending on the selected heterodienes and substituents in the naphthoquinone fragment providing various types of polycyclic systems [29–34] (Figure 2). It is also worth noting that Diels–Alder reactions of naphthoquinone derivatives as dienophiles make it possible to obtain some biologically active natural quinones, particularly angucyclinone antibiotics, which undergo stages of clinical trials [35]. Accordingly, the purpose of this work was to apply 1,4-naphthoquinone as the dienophile in *hetero*-Diels–Alder reactions for the synthesis of novel thiopyrano[2,3-*d*]thiazole derivatives. It is worth noting that thiopyrano[2,3-*d*]thiazole derivatives have shown a broad range of biological activities, such as anticancer [36–38], antioxidant [39], antitrypanosomal [40], anti-inflammatory [41], etc. The synthesized compounds were also evaluated for their primary anticancer activity, cytotoxicity, and DNA intercalation *in vitro*.

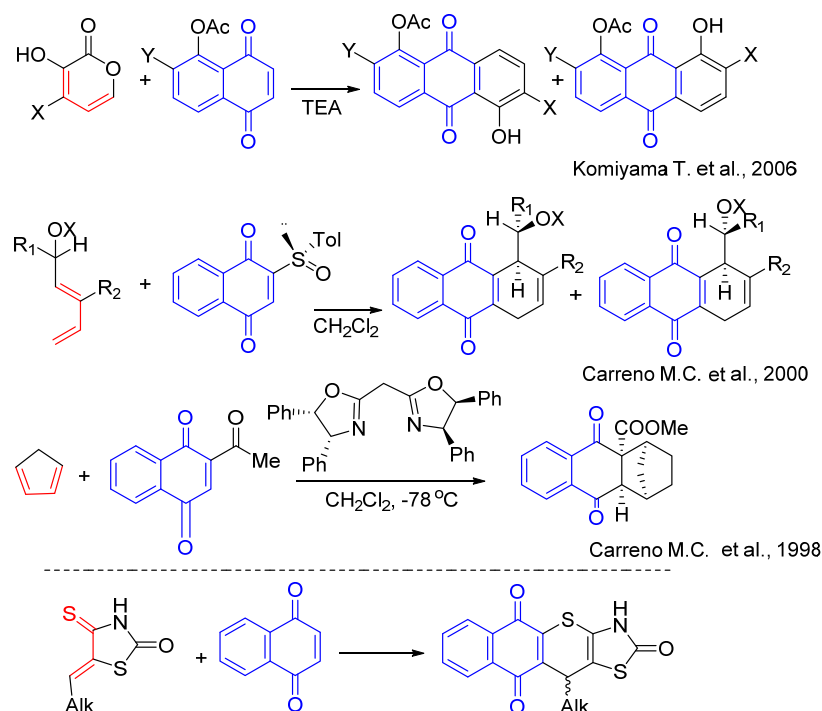


Figure 2. Background for targeted compound synthesis [29–31].

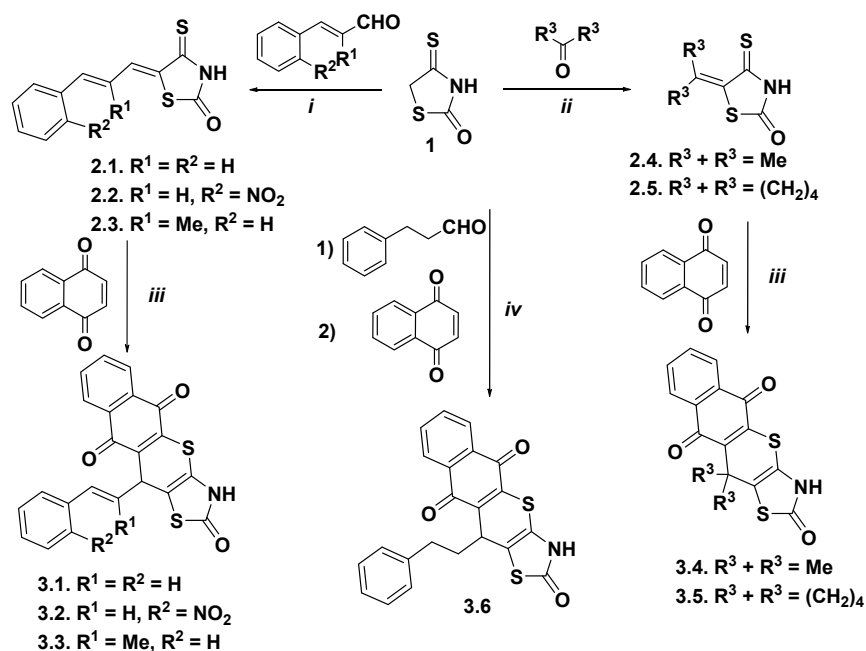
2. Results

2.1. Chemistry

The starting 5-aryllallylidene- and 5-(cyclo)alkylidene-4-thioxo-2-thiazolidinones, as heterodienes in the synthesis of target thiopyranothiazole derivatives, were synthesized via the Knoevenagel condensation of 4-thioxo-2-thiazolidinone (isorhodanine) and appropriate aldehydes or ketones using ethylenediammonium diacetate (EDDA) as the catalyst in ethanol medium. The *hetero*-Diels–Alder reaction was carried out in boiling acetic acid in the presence of a catalytic amount of hydroquinone as a side polymerization inhibitor, and target 11-substituted-3,5,10,11-tetrahydro-2*H*-benzo[6,7]thiochromeno[2,3-*d*][1,3]thiazole-2,5,10-triones **3.1–3.6** were obtained with good yields (Scheme 1). It should be noted that aliphatic aldehydes with isorhodanine react less actively with low yields, and the resulting 5-alkylidene-4-thioxo-2-thiazolidinones are quite difficult to isolate [42]. Accordingly, a three-component reaction of isorhodanine, aliphatic aldehyde, and dienophile was used to synthesize target thiopyrano[2,3-*d*]thiazoles. The reaction of isorhodanine, 3-phenylpropionaldehyde, and 1,4-naphthoquinone in acetonitrile in the presence of EDDA as catalyst afforded pure target derivative **3.6**. It is worth noting that during the *hetero*-Diels–Alder reaction, the products of [4+2]-cycloaddition undergo spontaneous oxidation (dehydrogenation) by excess naphthoquinone, which has been reported previously [38].

The structures of the synthesized compounds were elucidated by spectral data. Thus, protons of the naphthoquinone moiety in the ^1H NMR spectra of synthesized thiopyranoids showed characteristic signals at $\delta \sim 7.02\text{--}8.49$ ppm. The signal of the CH proton in the C-16 position appeared as a singlet or multiplet at 4.42–6.77 ppm. Protons attributed to the phenylpropionyl residue of **3.6** showed two multiplets at $\delta 1.94\text{--}2.62$ ppm. Low field ^1H NMR spectra gave signals in a range of 10.80–11.89 ppm, which were assigned to the signal of the amide proton. In the ^{13}C NMR spectra of the synthesized compounds, the signals observed at $\delta 166.9\text{--}185.3$ were assigned to the carbonyl group (C=O) of the naphthoquinone fragment (Figures S1–S12).

The structure of the synthesized 11-phenethyl-3,11-dihydro-2*H*-benzo[6,7]thiochromeno[2,3-*d*]thiazole-2,5,10-trione (**3.6**) was confirmed by X-ray diffraction analysis. The molecular structure and the atom-labeling Scheme are illustrated in Figure 3.



Scheme 1. Synthesis of thiopyrano[2,3-*d*]thiazoles containing a naphthoquinone moiety. Reagents and conditions: (i) isorhodanine 1 (10 mmol), appropriate aldehyde (10 mmol), EDDA (10 μ mol), methanol (10 mL), reflux, 10 min; r.t. 12 h, 77–80%; (ii) isorhodanine 1 (1.0 equiv), appropriate ketone (15–20 equiv), ethanolamine (2–3 drops), r.t., 1 h; 74–90%; (iii) comp. 2.1–2.5 (1.0 equiv), 1,4-naphthoquinone (2.0 equiv), hydroquinone, AcOH, reflux, 1 h, 69–81%; (iv) isorhodanine 1 (5.0 mmol), phenylpropionaldehyde (5.5 mol), 1,4-naphthoquinone (10.0 mmol), EDDA (5 μ mol), MeCN (10 mL), reflux, 2 h, 70%.

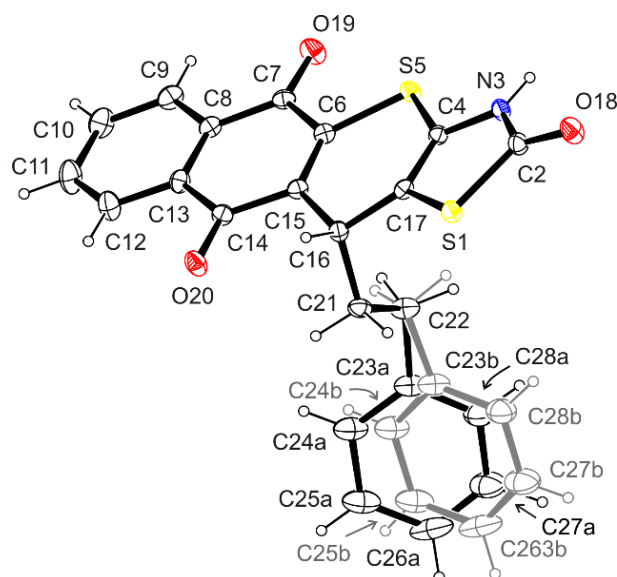


Figure 3. ORTEP view of the molecule of 3.6 showing the atomic labeling Scheme. Non-H atoms are drawn as 30% probability displacement ellipsoids and H atoms are drawn as spheres of an arbitrary radius.

The compound has a rigid tetracyclic system of 3,11-dihydro-2*H*-benzo[6,7]thiochromeno[2,3-*d*]thiazole-2,5,10-trione with the planar or approximately planar thiazolin-2-one and naphthalene-1,4-dione ring moieties (r.m.s. deviation 0.0041 and 0.0209 Å, respectively), and the slightly puckered 4*H*-thiopyran ring (r.m.s. deviation 0.0846 Å).

Within the thiazolin-2-one system, the presence of a secondary amide group was noted. The position of the hydrogen atom bound to the N-3 atom was determined from the difference Fourier map and freely refined. Its location in the mentioned position was confirmed by the hydrogen bond N3–H3 \cdots O18ⁱ [Donor–H: 0.89(4) Å, H \cdots Acceptor: 1.89(4) Å, Donor \cdots Acceptor: 2.744(4) Å, Donor–H \cdots Acceptor: 160(4)°], in which the carbonyl oxygen atom plays the role of the proton acceptor.

Our studies have shown that in the 3,11-dihydro-2*H*-benzo[6,7]-thiochromeno[2,3-*d*]thiazole-2,5,10-trione ring system there are double bonds between the nodal C-4/C-17 and C-6/C-15 atoms. The found interatomic distances C4–C17 [1.339 (4) Å] and C6–C15 [1.349(4) Å] are close to the literature length of the double C–C bond [1.331(1) Å] [43].

Structural investigations have shown that in the crystal, the phenyl ring of the phenethyl residue at the stereogenic atom C-16 occupies two alternative positions, marked *a* and *b*, as a result of swing motion and simultaneous rotation of the ring around the C23–C26 axis. The angle C23*a*–C22–C23*b* and the dihedral angle Ph_*a*–Ph_*b* found are 17.2(4) and 26.9(3)°, respectively. Occupancy factors for alternative positions *a* and *b* of the phenyl ring are 0.5.

The arrangement of the phenethyl residue is described with torsion angles C4–C17–C16–C21, C17–C16–C21–C22, and C16–C21–C22–C23*a*/23*b*, which reveal values of 104.1(3), –67.7(3), and –170.3(4)/171.9(4)°. Moreover, the alternative phenyl rings *a* and *b* belonging to phenethyl moiety form with the mean plane of 4*H*-thiopyran ring the dihedral angles of 68.8(2) and 60.8(2)°, respectively.

2.2. Biological Evaluation

2.2.1. Cytotoxicity Activity Screening

Considering the results of previous studies of fused thiazolidinones and their analogs, a series of thiopyrano[2,3-*d*]thiazoles with naphthoquinone fragments in the structure were studied for their anticancer activity. Thus, synthesized thiopyranothiazole derivatives **3.5** and **3.6** were selected by the National Cancer Institute (NCI), U.S., for their anticancer activity at 10 μM concentration toward a panel of sixty cancer cell lines representing nine different types (leukemia, melanoma, lung, colon, CNS, ovarian, renal, prostate, and breast cancers) (Figures S13–S14). Selection for screening based on new derivatives' ability to add diversity to the NCI small molecules collection and anticancer assays were performed according to the NCI guidelines and protocols previously described [44–46]. The compounds were added at the mentioned concentration, and the cell cultures were incubated for 48 h. The results for each compound were reported as the growth percent (GP%) of treated cells compared with untreated control cells. The screening results are shown in Table 1.

Table 1. Anticancer Screening Data in Concentration of 10 μM.

Compound NSC	Mean Growth, %	Range of Growth, %	Most Sensitive Cell Line Growth, % (Cancer Line/Type)
3.5 748457	88.33	51.21 to 126.93	53.82 (RPMI-8226/Leukemia)
			59.89 (SR/Leukemia)
			54.98 (EKVX/Non-Small Cell Lung Cancer)
			55.15 (IGROV1/Ovarian Cancer)
			55.54 (UO-31/Renal Cancer)
			51.21 (T-47D/Breast Cancer)
3.6 831850	90.58	45.25 to 130.11	57.17 (LOX IMVI/Melanoma)
			45.25 (MALME-3M/Melanoma)
			52.87 (MDA-MB-435/Melanoma)
			51.76 (UO-31/Renal Cancer)
			58.83 (MCF7/Breast Cancer)

Table 1. Cont.

Compound NSC	Mean Growth, %	Range of Growth, %	Most Sensitive Cell Line Growth, % (Cancer Line/Type)
Doxorubicin 759155	−20.30	−86.40 to 72.90	−81.60 (COLO-205/ Colon Cancer)
			−76.10 (SNB-75/ Central Nervous System Cancer)
			−71.60 (M14/ADR-RES/ Melanoma)
			−82.60 (MDA-MB-435/Melanoma)
			−82.60 (SK-MEL-2/Melanoma)
			−86.40 (SK-MEL-5/Melanoma)
			−75.10 (A498/ Renal Cancer)

The studied naphthoquinone-substituted thiopyrano[2,3-*d*]thiazoles demonstrated inhibition of tested cancer cell lines growth in the in vitro screening. The GP of breast cancer T-47D cells was 51.21% under treatment with compound **3.5**, and the GP of melanoma MALME-3M cells was 45.25% under treatment with compound **3.6**.

We continued the cytotoxicity study of synthesized derivatives **3.1–3.6** toward tumor and pseudo-normal cells in vitro. The MTT cell viability assay was performed 72 h after cells treatment with various concentrations of studied compounds and doxorubicin, a reference drug. The cell viability and the IC₅₀ values are shown in Figure 4 and Table 2. The most active was compound **3.6**, and leukemic cell lines were the most sensitive to its action. It was cytotoxic to Jurkat T-leukemia cells at all tested concentrations with the half-maximal inhibitory concentration (IC₅₀) of 0.76 μM. The THP-1 cells, monocytes isolated from peripheral blood from an acute monocytic leukemia patient [47], were also sensitive to the **3.6** treatment. The IC₅₀ of this compound was 7.94 μM. The **3.6** inhibited the viability of epidermoid carcinoma (KB3-1 and its ABCB1-overexpressing subline KBC-1) and colon carcinoma (HCT116wt and its p53 knockdown subline HCT116 p53^{-/-}) cells. It is known that ABCB1 (P-glycoprotein), MRP1/ABCC1 (multidrug resistance protein 1), and BCRP/BCG2 (breast cancer resistance protein) have been reported to be key players in resistance to chemotherapy [48]. It should be noted that the **3.6** demonstrated a pronounced growth inhibition effect on KBC-1 (IC₅₀ = 12.81 μM). The IC₅₀ of **3.6** was 27.66 μM for KB3-1 cells. We found significantly lower IC₅₀ values of **3.2**, **3.4**, and **3.6** for HCT116wt compared with those for the HCT116 p53^{-/-} cell line. The IC₅₀ ranged from 5.54 to 6.81 μM and from 12.34 to >50 μM, respectively. Thus, the p53 status of colon carcinoma cells influenced the anti-tumor effects of the studied 3,5,10,11-tetrahydro-2*H*-benzo[6,7]thiochromeno[2,3-*d*][1,3]thiazole-2,5,10-trione. The p53 has diverse mutations in almost all human tumors, stimulating their hyper-proliferation, invasion/metastasis, and thus, influencing the potency of various chemotherapeutics (i.e., platins and anti-metabolites). The p53-deficient or p53-mutant tumors often possessed a more aggressive phenotype and more pronounced chemo- and radio-resistance [49]. Based on our findings, one can assume a p53-dependent mode of action for **3.6** toward colon cancer cells.

Table 2. Influence of Compounds and 1,4-NQ on the Growth of Individual Tumor Cell Lines.

Cell Line	IC ₅₀ , μM							
	3.1	3.2	3.3	3.4	3.5	3.6	1,4-NQ	Dox
KB3-1	36.99	39.22	28.81	26.01	>50	27.66	20.74	0.73
KBC-1	ND	ND	ND	ND	ND	12.81	8.33	1.97
Jurkat	ND	ND	ND	ND	ND	0.76	ND	0.67
THP-1	ND	ND	ND	ND	ND	7.94	ND	13.97
HCT116wt	29.19	6.81	15.84	5.54	43.55	6.37	ND	0.07
HCT116 p53 ^{-/-}	40.34	>50	11.09	25.22	>50	12.34	ND	0.58
MCF-7	9.19	8.47	26.75	34.34	>50	8.94	ND	0.63
HaCaT	ND	ND	ND	ND	ND	>100	ND	0.80

Table 2. Cont.

Cell Line	IC ₅₀ , μM							
	3.1	3.2	3.3	3.4	3.5	3.6	1,4-NQ	Dox
J774.2	24.44	0.74	30.52	11.07	>50	9.57	ND	0.97
Isolated lymphocytes	ND	ND	ND	ND	ND	58.66	62.93	1.00
K562	43.72	26.00	13.00	7.11	>50	25.67	ND	0.62

ND—not determined.

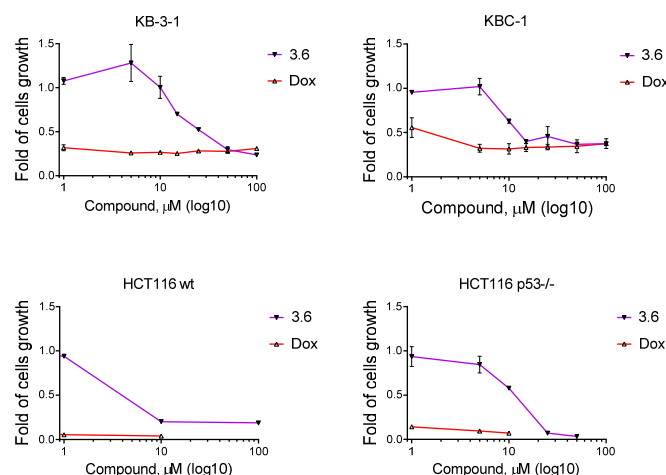


Figure 4. The viability curves of epidermoid (KB3-1, KBC-1) and colon (HCT116wt, HCT116 p53^{-/-}) cells under derivative 3.6 and doxorubicin treatment. The anti-proliferative activity of studied compounds was analyzed by MTT assay after 72 h of cell exposure. Data presented as $M \pm SD$, $n = 3$.

Derivatives 3.1, 3.2, and 3.6 possessed an anti-proliferative effect on MCF-7 (hormone-dependent, estrogen, and progesterone receptor positive) cells with a similar IC₅₀ of 9.19, 8.47, and 8.94 μM , respectively [50]. K562 cells were sensitive to compounds 3.3 and 3.4, with an IC₅₀ of 13.00 and 7.11 μM , respectively. Doxorubicin was more cytotoxic for epidermoid, colon, breast carcinoma, and melanoma cells (Figure 4, Table 2). Compound 3.5 showed weak activity on cell lines used in our work. A reference compound was also used, 1,4-naphthoquinone (1,4-NQ), with weak activity towards KB3-1 and KBC-1 cell lines (IC₅₀ 20.74 and 8.33 μM , respectively).

The 3.6 showed low toxicity in human keratinocytes of the HaCaT line. The IC₅₀ of 3.6 was >100 μM for HaCaT cells. The isolated normal human peripheral blood lymphocytes and murine macrophages of the J774.2 line were more sensitive to 3.6 treatment. It induced a 50% reduction in the viability of isolated normal human lymphocytes at 58.66 μM . The 3.6 reached the IC₅₀ value at 9.57 μM for the J774.2 macrophage cell line. The 3.6 derivative caused a moderate reduction in the viability of HaCaT, J774.2 cell lines, and isolated normal human lymphocytes. The blood-derived cells were more sensitive to the 3.6 treatment. Doxorubicin reduced the survival of pseudo-normal cells and isolated normal lymphocytes at the IC₅₀ value of 0.8–1.0 μM (Figure 5, Table 2).

Compound 3.6 possessed a high anti-proliferative effect on selected tumor cells and moderate toxicity on pseudo-normal ones. Thus, it was chosen for further experimental research in vitro.

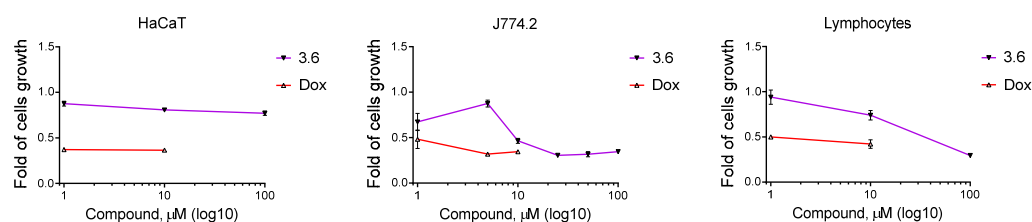


Figure 5. The viability of human keratinocytes of HaCaT line, murine macrophages of J774.2 line, and isolated normal human peripheral blood lymphocytes upon exposure to different concentrations of compound 3.6 and doxorubicin (Dox) for 72 h. The anti-proliferative activity of studied compounds was analyzed by MTT assay after 72 h of cells exposure. Data presented as $M \pm SD$, $n = 3$.

2.2.2. Reactivity with Reduced Glutathione (GSH)

The reactivity of unmetabolized compound 3.6 was assessed in the test with the model soft nucleophile reduced glutathione (GSH). It has been found that after incubation with 3.6, the level of GSH decreases and does not increase with adding sodium borohydride, which suggests the formation of covalent GS-adducts that are not reduced to GSH with sodium borohydride, unlike oxidized glutathione GSSG (Figure 6).

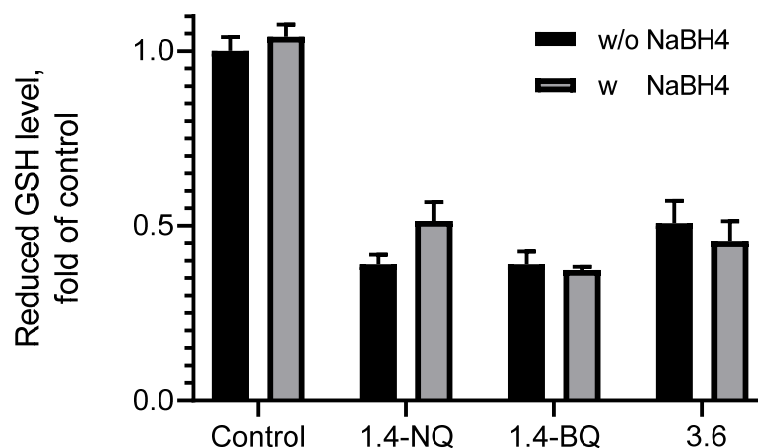


Figure 6. Reduced glutathione (GSH) level.

2.2.3. Cellular Morphology of KB3-1 Cells Induced by Compound 3.6

To elucidate the primary death mechanisms in the treated cells with the 3.6 derivative, we assessed apoptosis by DNA laddering assay, fluorescent microscopy after cell staining with Hoechst-33342, DNA interacting spectroscopic, and DNA/methyl green replacement assays.

The 3.6 caused significant cytomorphological alterations in KB3-1 cells, which were found to be shrunk, with condensed chromatin and membrane blabbing (Figure 7B) compared to the control (Figure 7A). One can also see giant KB3-1 cells with abnormal nuclei and looser chromatin (Figure 7B). The mitotic catastrophe may occur during or after aberrant mitosis. Mitotic catastrophe has been reported as a special example of apoptosis affecting mitochondrial membrane permeabilization and caspase activation [51]. The control KB3-1 cells exhibited properly shaped intact nuclei. Doxorubicin caused chromatin condensation and membrane blabbing (Figure 7C). Thus, compound 3.6 induced pro-apoptotic cytomorphological changes in treated KB3-1 cells. As shown in Figure 7B, compound 3.6 was able to red fluorescence (DIC + Red channel) in the cells, similar to doxorubicin (Figure 7C), and was more concentrated in the nucleus area.

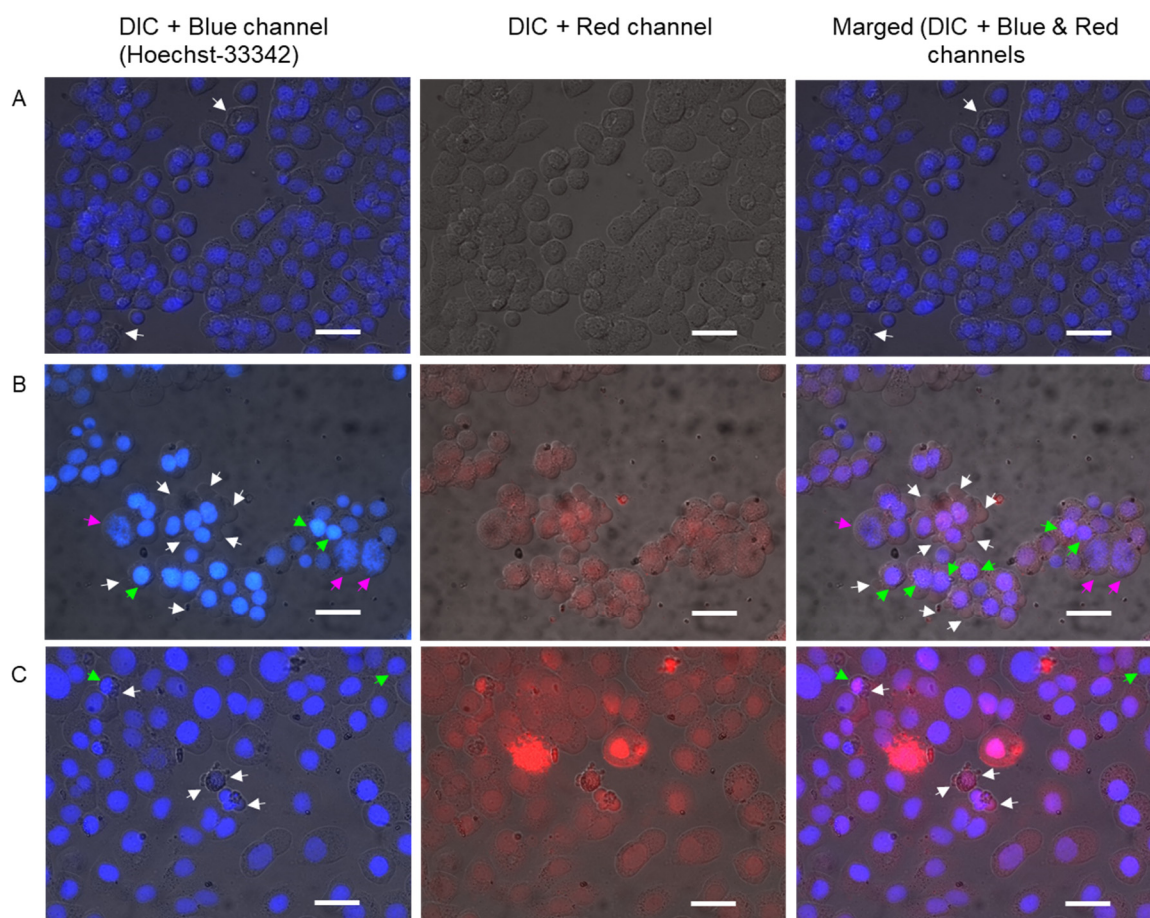


Figure 7. Photomicrographs of KB3-1 cells analyzed through Hoechst 33342 staining following 24 h exposure to studied compounds: (A)—control (untreated) cells; (B)—cells treated with **3.6** (1 μ M); (C)—cells treated with doxorubicin (1 μ M). Bar equals 20 μ m.

2.2.4. DNA Laddering under Treatment of **3.6**

In the presence of compound **3.6**, we did not detect a typical apoptotic laddering in Jurkat cells (Figure 8). One can see that compound **3.6** at 1 μ M induced slight laddering of DNA. The **3.6** at 2.5 μ M and 5 μ M induced necrotic degradation of DNA. We assumed that the **3.6** at 10 μ M and 25 μ M induced extreme DNA fragmentation that could not be seen on the gel.

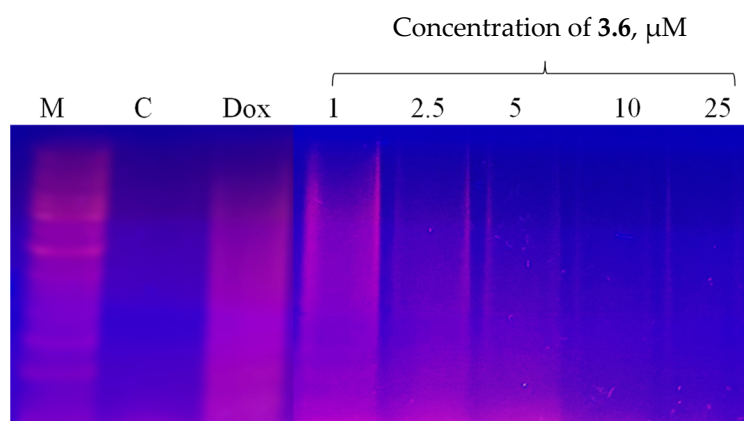


Figure 8. DNA ladder in KB3-1 cells following 24 h exposure to the compound **3.6** and doxorubicin (Dox, 1 μ M).

Compound **3.6** induced both apoptotic and necrotic death of KB3-1 cells. Doxorubicin at 0.5 μM induced more necrotic changes in treated Jurkat cells than apoptotic ones (Figure 8).

2.2.5. DNA Interacting Ability of Compound 3.6

The method investigates conformational changes in the DNA; for example, when DNA is exposed to an intercalating, alkylation, or other classes of DNA-binding agents. It is based on the oxidative reaction of potassium permanganate with pyrimidine bases. Compounds that interact with DNA distort its duplex structure, thus exposing pyrimidine bases for oxidation by KMnO_4 , which generates products that can be detected by spectrophotometry [52]. Different classes of DNA-binding compounds can be studied in such a way. Data obtained from samples with DNA incubated with the tested compound **3.6** showed a strong time and concentration-dependent increase in the oxidation level compared with control DNA (without the studied compound). Net A405 ranged from 0.00 to 0.50 in the presence of the compound, and Net A405 ranged from 0.02 to 0.045 in the control case (Figure 9). The obtained results indicated that compound **3.6** interacts in some way with DNA.

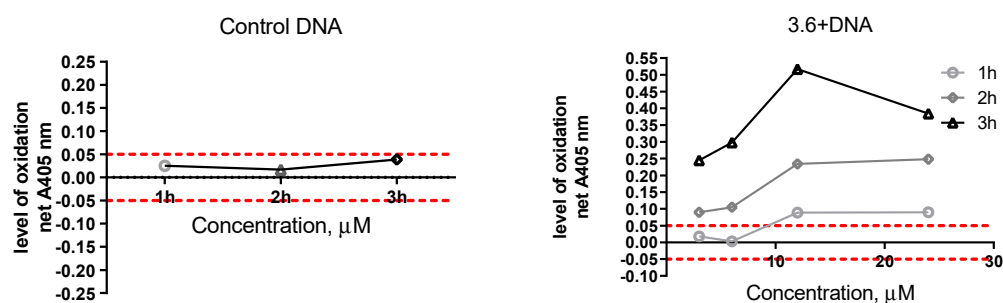


Figure 9. Variation in the net change of absorbance with increasing concentration of studied compound at different time periods. The control solution includes DNA, water, and KMnO_4 . The studied sample included DNA, compound **3.6**, and KMnO_4 .

2.2.6. DNA/Methyl Green Replacement Assay

In addition, we used DNA/methyl green colorimetric assay to study the possible interaction of compound **3.6** in DNA. Methyl green is found to be a DNA major-groove binding compound [53] and reversibly binds polymerized DNA. This assay was used to measure the displacement of methyl green from DNA by compounds with the ability to intercalate DNA [54]. Tested compound **3.6** could intercalate between two complementary base pairs in double-stranded DNA, and, dependent on concentration, the percentage of methyl green replacement ranged from 35.00 to 39.64% (Figure 10). Indeed, 1,4-NQ showed a stronger ability to methyl green replacement; in concentration 1 μM it displaced 65% of methyl green. Doxorubicin, which was used as a positive control, in concentration 1 μM , had a similar effect to compound **3.6**, but in concentration 10 μM replaced methyl green as being two times more effective. Together with data obtained in through spectroscopic assay, and red fluorescence in the nucleus area (morphology data), this result indicated that one of the possible mechanisms of action of compound **3.6** is DNA intercalation.

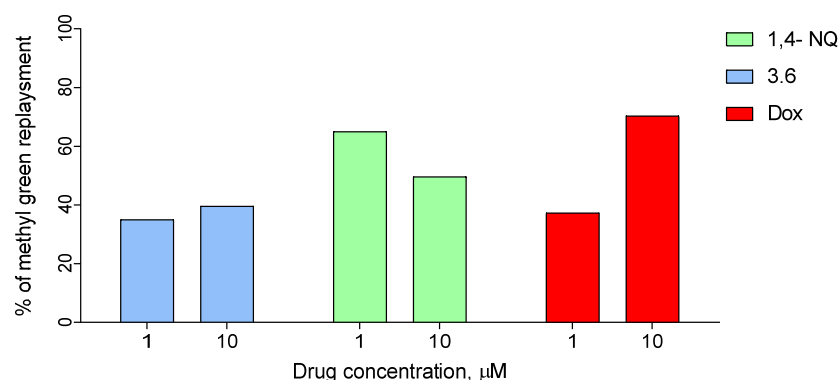


Figure 10. Replacement of methyl green, intercalated to salmon sperm DNA, by the compound **3.6**, 1,4-NQ, and doxorubicin (positive control).

3. Materials and Methods

3.1. General Information

All materials were purchased from commercial sources and used without purification. Melting points were measured in open capillary tubes and were uncorrected. The elemental analyses were performed using a Thermo Scientific FlashSmart Elemental Analyzer. The ^1H and ^{13}C NMR spectra were recorded on a Varian Gemini (^1H at 400 and ^{13}C at 100 MHz) instrument in $\text{DMSO-}d_6$. Chemical shifts (δ) were given in ppm units relative to tetramethylsilane as reference (0.00). The purity of all obtained compounds was checked by TLC on Silufol-254 plates (Eluent EtOAc/ Benzene 1:2). The starting 5-ylidene-4-thioxo-2-thiazolidinones 2.1–2.5 were obtained according to the method previously described [41,55].

Human colon carcinoma HCT116 cells, human breast adenocarcinoma cells of MCF-7 line, human T-leukemia Jurkat cells, human chronic myelogenous leukemia K562 cells, and human keratinocytes of HaCaT line were from the Cell Collection of R.E. Kavetsky Institute of Experimental Pathology, Oncology and Radiobiology (Kyiv, Ukraine). Murine macrophages of J774.2 line were a generous gift from Professor Sir John Vane (William Harvey Research Institute, London, UK) via Professor Janusz Marcinkiewicz (Jagiellonian University Medical College, Krakow, Poland). Human colon carcinoma HCT116 p53^{-/-} cells with knockdown of P53 gene, as well as human epidermoid cervix carcinoma KB3-1 cells and its ABCB1-overexpressing subline KBC-1, were kindly provided by Professor W. Berger (Institute of Cancer Research, Medical University of Vienna, Austria). The phenotype of this cell line was stable, as periodically determined by Western blot analysis. Human leukemia monocytic THP-1 cells were kindly provided by Professor M. Herrmann (Department of Internal Medicine, Institute for Clinical Immunology and Rheumatology, University of Erlangen-Nuremberg, Germany). Cells were cultured in DMEM or RPMI-1640 medium supplemented with 10% fetal bovine serum (all were purchased from Biowest, Nuaille, France) at 37 °C in a humidified atmosphere containing 5% CO_2 .

3.2. Synthesis of 3,11-Dihydro-2H-benzo[6,7]thiochromeno[2,3-d]thiazole-2,5,10-triones **3.1–3.5**

A mixture of appropriate 5-alkyl/arylallylidene/-4-thioxo-2-thiazolidinone (10 mmol) and 1,4-naphthoquinone (20 mmol) was refluxed for 1 h with a catalytic amount of hydroquinone (2–3 mg) in glacial acetic acid (10 mL), and then left overnight at room temperature. The precipitated crystals were filtered off, washed with methanol (5–10 mL), and recrystallized from the appropriate solvent.

11-Styryl-3,11-dihydro-2H-benzo [6,7]thiochromeno [2,3-d]thiazole-2,5,10-trione (3.1). Yield 70%, mp 338–340 °C (DMF:EtOH). ^1H NMR (400 MHz, $\text{DMSO-}d_6$): δ 6.77 (s, 1H, CH), 7.53–7.63 (m, 6H, CH, arom.), 7.69 (t, 1H, J = 7.8 Hz, arom.), 7.73 (t, 1H, J = 8.2 Hz, arom.), 8.12 (d, 1H, J = 16.4 Hz, CH), 8.24 (d, 1H, J = 8.4 Hz, arom.), 8.39 (d, 1H, J = 8.4 Hz, arom.), 11.04 (s, 1H, NH). ^{13}C NMR (100 MHz, $\text{DMSO-}d_6$): δ 36.2, 95.8, 118.7, 119.6, 122.4, 123.5, 126.6, 127.7, 128.1, 129.1, 129.2, 129.9, 131.4, 131.8, 147.8, 156.2, 175.2, 177.2, 179.7 ESI-MS

m/z 404 (M + H)⁺. Anal.Calcd for C₂₂H₁₃NO₃S₂: C, 65.49; H, 3.25; N, 3.47. Found: C, 65.64; H, 3.08; N, 3.63.

11-(2-Nitrostyryl)-3,11-dihydro-2H-benzo[6,7]thiochromeno[2,3-d]thiazole-2,5,10-trione (3.2). Yield 69%, mp 330–332 °C (DMF:EtOH). ¹H NMR (400 MHz, DMSO-d₆): δ 6.02–6.08 (m, 1H, CH), 7.66 (t, 2H, J = 8.4 Hz, arom.), 7.74–7.77 (m, 2H, arom.), 7.89–7.93 (m, 1H, arom.), 8.10 (dd, 2H, J = 8.2, 16.0 Hz, 2CH), 8.18 (d, 1H, J = 8.4 Hz, arom.), 8.29 (d, 2H, J = 8.2 Hz, arom.), 11.83 (s, 1H, NH). ¹³C NMR (100 MHz, DMSO-d₆): δ 31.6, 98.1, 114.4, 118.8, 122.6, 125.1, 130.3, 132.6, 134.4, 134.9, 137.1, 139.1, 141.9, 144.2, 146.6, 149.7, 173.5, 174.9, 178.5. ESI-MS m/z 449 (M + H)⁺. Anal.Calcd for C₂₂H₁₂N₂O₅S₂: C, 58.92; H, 2.70; N, 6.25. Found: C, 59.07; H, 2.82; N, 6.12.

11-(2-Phenylprop-1-en-1-yl)-3,11-dihydro-2H-benzo[6,7]thiochromeno[2,3-d]thiazole-2,5,10-trione (3.3). Yield 80%, mp > 350 °C (DMF:EtOH). ¹H NMR (400 MHz, DMSO-d₆): δ 0.96 (s, 3H, CH₃), 5.77 (s, 1H, CH), 7.41–7.44 (m, 1H, arom.), 7.50–7.56 (m, 2H, CH, arom.), 7.60–7.65 (m, 1H, arom.), 7.69–7.73 (m, 3H, arom.), 7.79–7.82 (m, 1H, arom.), 8.28–8.32 (m, 1H, arom.), 8.46–8.49 (m, 1H, arom.), 10.80 (s, 1H, NH). ¹³C NMR (100 MHz, DMSO-d₆): δ 17.1, 29.2, 86.1, 108.6, 122.4, 122.6, 125.4, 125.7, 126.2, 126.3, 126.4, 127.4, 128.0, 128.5, 144.4, 146.7, 164.2, 166.9, 177.6. ESI-MS m/z 418 (M + H)⁺. Anal.Calcd for C₂₃H₁₅NO₃S₂: C, 66.17; H, 3.62; N, 3.35. Found: C, 66.27; H, 3.40; N, 3.49.

11,11-Dimethyl-3,11-dihydro-2H-benzo[6,7]thiochromeno[2,3-d]thiazole-2,5,10-trione (3.4). Yield 81%, mp 230–232 °C (DMF:EtOH). ¹H NMR (400 MHz, DMSO-d₆): δ 1.73 (s, 3H, CH₃), 1.89 (s, 3H, CH₃), 7.82 (t, 1H, J = 7.6 Hz, arom.), 7.88 (d, 1H, J = 7.3 Hz, arom.), 7.94–8.02 (m, 2H, arom.), 11.65 (s, 1H, NH). ¹³C NMR (100 MHz, DMSO-d₆): δ 21.0, 29.7, 106.3, 114.6, 125.8, 126.9, 135.1, 142.8, 146.2, 170.0, 172.0, 180.7. ESI-MS m/z 330 (M + H)⁺. Anal.Calcd for C₂₂H₁₅NO₃S₂: C, 65.17; H, 3.73; N, 3.45. Found: C, 65.24; H, 3.61; N, 3.62.

Spiro[benzo[6,7]thiochromeno[2,3-d]thiazole-11,1'-cyclopentane]-2,5,10(3H)-trione (3.5). Yield 72%, mp 231–233 °C (AcOH). ¹H NMR (400 MHz, DMSO-d₆): δ 2.14 (br.s, 2H, CH₂), 2.39 (br.s, 2H, CH₂), 2.81 (m, 4H, 2*CH₂), 7.84 (m, 2H, arom.), 8.05 (m, 2H, arom.), 11.70 (s, 1H, NH). ¹³C NMR (100 MHz, DMSO-d₆): δ 21.7, 31.2, 45.5, 106.5, 122.3, 127.8, 134.6, 136.3, 138.3, 143.3, 150.3, 176.0, 177.7, 185.3. ESI-MS m/z 356 (M + H)⁺. Anal.Calcd for C₁₆H₁₁NO₃S₂: C, 58.34; H, 3.37; N, 4.25. Found: C, 58.21; H, 3.52; N, 4.16.

3.3. Synthesis of

11-Phenethyl-3,11-dihydro-2H-benzo[6,7]thiochromeno[2,3-d]thiazole-2,5,10-trione 3.6

A mixture of isorhodanine (5 mmol), phenylpropionaldehyde (5.5 mmol), and 1,4-naphthoquinone (10 mmol) was heated at reflux for 2 h in MeCN (10 mL) in the presence of the catalytic amount of ethylenediaminediacetic acid. After cooling, the precipitate was filtered off, washed, and recrystallized from the appropriate solvent. Yield 70%, mp 200–202 °C (DMF:EtOH). ¹H NMR (400 MHz, DMSO-d₆): δ 1.94 (m, 2H, CH₂), 2.62 (m, 2H, CH₂), 4.42 (m, 1H, CH), 7.02 (m, 1H, arom.), 7.07–7.14 (m, 4H, arom.), 7.78–7.93 (m, 2H, arom.), 7.94–8.06 (m, 2H, arom.), 11.89 (s, 1H, NH). ¹³C NMR (100 MHz, DMSO-d₆): δ 31.6, 34.3, 36.5, 107.0, 117.1, 126.2, 126.5, 127.1, 128.5, 128.6, 131.4, 131.9, 134.3, 135.3, 137.0, 141.5, 143.7, 171.3, 180.3, 180.8. ESI-MS m/z 406 (M + H)⁺. Anal.Calcd for C₁₆H₁₁NO₄S₂: C, 55.64; H, 3.21; N, 4.06. Found: C, 55.51; H, 3.09; N, 4.19.

3.4. Crystal Structure Determination of

11-Phenethyl-3,11-dihydro-2H-benzo[6,7]thiochromeno[2,3-d]thiazole-2,5,10-trione Dimethylaminoformamide Hemisolvate (3.6·1/2DMF)

Compound **3.6** was recrystallized from DMF by slow evaporation at room temperature.

Crystal data of compound 3.6 C₂₂H₁₅NO₃S₂, 0.5(C₃H₇NO), *M_r* = 442.02, monoclinic, space group C2/c, *a* = 19.9599(5), *b* = 8.08330(10), *c* = 26.8363(6) Å, β = 111.649(3)°, *V* = 4024.40(16) Å³, *Z* = 8 (*Z'* = 1), *D_{calc}* = 1.459 g/cm³, μ = 2.661 mm⁻¹, *T* = 130.0(1) K.

Data collection of compound 3.6. A brown lath crystal (DMF) of 0.45 × 0.12 × 0.08 mm was used to record 9137 (Cu Kα-radiation, θ_{max} = 76.22°) intensities on a Rigaku SuperNova Dual Atlas diffractometer [56] using mirror monochromatized Cu Kα-radiation from a high-flux microfocus source (λ = 1.54184 Å). Accurate unit cell parameters were determined

by least-squares techniques from the θ values of 7380 reflections, θ range 4.42–75.95°. The data were corrected for Lorentz, polarization, and for absorption effects [56]. The 4126 total unique reflections ($R_{\text{int}} = 0.0146$) were used for structure determination.

Structure solution and refinement of compound 3.6. The structure was solved by a dual space algorithm (SHELXT) [57] and refined against F^2 for all data (SHELXL) [58]. The position of the H atom bonded to N atom was obtained from the difference Fourier map and was freely refined. The remaining H atoms were positioned geometrically and were refined within the riding model approximation: C–H = 0.99 Å (CH₂), 1.00 Å (Csp³H), 0.95 Å (Csp²H) and $U_{\text{iso}}(\text{H}) = 1.2U_{\text{eq}}(\text{C})$. Final refinement converged with $R = 0.0584$ (for 4079 data with $F^2 > 4\sigma(F^2)$), $wR = 0.1319$ (on F^2 for all data), and $S = 1.144$ (on F^2 for all data). The largest difference peak and hole was 0.378 and $-0.421 \text{ e}\text{\AA}^3$. The solvent masks procedure implemented in OLEX2 [59] was employed to remove disordered solvent molecules that could not be reliably modeled. The solvent radius was set to 1.2 Å; calculated total potential solvent-accessible void volume and electron counts per unit-cell were: 484 Å³ and 148.

The molecular illustration was drawn using ORTEP-3 for Windows [60]. Software used to prepare material for publication was OLEX2 [59] and PLATON [61].

The supplementary crystallographic data were deposited at the Cambridge Crystallographic Data Centre (CCDC), 12 Union Road, Cambridge, CB2 1EZ (UK) [phone, (+44) 1223/336-408; fax, (+44) 1223/336-033; e-mail, deposit@ccdc.cam.ac.uk; World Wide Web, <http://www.ccdc.cam.ac.uk>, accessed on 2 October 2022 (deposition no. CCDC 2210721)].

3.5. Cytotoxic Activity against Malignant Human Tumor Cells According to the DTP NCI Protocol

Anticancer in vitro assay was performed on the human tumor cell lines panel derived from nine neoplastic diseases by the protocol of the Drug Evaluation Branch, National Cancer Institute, Bethesda, MD, USA [44–46]. Tested compounds were added to the culture at a single concentration (10^{-5} M), and the cultures were incubated for 48 h. Endpoint determinations were made with a protein binding dye, sulforhodamine B. Results for each tested compound were reported as the GP% of the treated cells compared to untreated control cells. GP% was spectrophotometrically evaluated vs. controls not treated with test agents.

3.6. MTT Cell Viability Assay

MTT assay was used to examine the viability of tumor and pseudo-normal cells after their treatment with studied thiopyrano[2,3-*d*]thiazole derivatives and doxorubicin (Actavis S.R.L., Bucharest, Romania). Cells were seeded in 96-well plates at a density of $3\text{--}5 \times 10^3$. After 24 h, cells were treated with compound 3.10, 1,4-NQ (0.1–100 µM), and doxorubicin (0.1–100 µM). After incubation for 72 h, MTT reagent (Sigma-Aldrich, St. Louis, MO, USA) was added to each well, according to the Sigma-Aldrich protocol. An absorbance Reader BioTek ELx800 (BioTek Instruments, Inc., Winooski, VT, USA) was used to measure the reaction product.

3.7. Reduced Glutathione (GSH) Level Assay

In model experiments, 1 mM of GSH and 1 mM of compounds in 0.1 M phosphate buffer (pH 7.4) were incubated for 1 h at 37 °C, and then the level of GSH was determined spectrophotometrically at 412 nm based on the reduction of 5,5'-dithio-bis(2-nitrobenzoic acid) to form the yellow derivative 5'-thio-2-nitrobenzoic acid. Oxidized glutathione GSSG in samples was reduced to GSH with sodium borohydride [62].

3.8. Spectroscopic DNA Interaction Assay

A spectroscopic DNA interaction study was performed as previously described [63]. salmon sperm DNA (Sigma-Aldrich, USA) was diluted in Milli-Q water at 4 °C for 24 h at 1.65 mg/mL. Tested compounds were dissolved in acetone. After 1 h of incubation of DNA and compound, KMnO₄ was added to a final concentration of 0.3 mM and the absorbance

at 405 nm was measured (Absorbance Reader BioTek ELx800) (BioTek Instruments, Inc., Winooski, VT, USA) in different periods up to 3 h. Appropriate controls of DNA alone and compound alone were included, and these Abs values were subtracted from the test sample to provide the net change in absorbance (NetAbs). DNA-binding compounds were defined as such where the net change in absorbance was >0.05 or <-0.05 , and DNA non-binding compounds ranged from 0.05 to -0.05 .

3.9. DNA/Methyl Green Colorimetric Assay

The capacity of the tested compounds to intercalate into salmon sperm DNA was determined using the methyl green assay. Briefly, salmon sperm DNA (10 mg/mL) was incubated for 1 h at 37 °C with 15 μ L of methyl green solution (1 mg/mL in H₂O). The compounds were added at concentrations 1 and 10 μ M/mL and incubated at 37 °C in the dark for 2 h. Reduction of the absorbance of methyl green at 642 nm induced by the test compounds was measured with a multiplate reader, Plate Reader BioTek Lx80 (BioTek Instruments, Inc., Winooski, VT, USA). Doxorubicin, a well-known intercalating agent, was used as a positive control.

3.10. DNA Extraction and Gel Electrophoresis

DNA extraction and gel electrophoresis were performed as described by Herrmann and others. Jurkat cells were collected by centrifugation; lysed in a lysis buffer (1% NP-40 in 20 mM EDTA, 50 mM Tris-HCl, pH 7.5; 10 μ L per 10⁶ cells, minimum 50 μ L). After centrifugation for 5 min at 1600 \times g, the supernatant was collected and the extraction was repeated with the same amount of lysis buffer. Supernatants were brought to 1% SDS and treated for 2 h with RNase A (final concentration 5 μ g/mL) at 56 °C. Then, proteinase K was added (final concentration 2.5, μ g/mL) and incubated for 2 h at 37 °C. After adding 1/2 volume of 10 M ammonium acetate, the DNA was precipitated with 2.5 vol. Ethanol, dissolved in gel loading buffer, and separated by electrophoresis in 1% agarose gels containing Ethidium bromide (at 70 V) [64].

3.11. The Fluorescence Microscopy of Cells

The KB3-1 cells were seeded in 24-well plates at 5×10^5 /mL and then treated for an additional 24 h with compound 3.10 (1 μ M) and doxorubicin (1 μ M). Cells were stained with 0.2–0.5 μ g/mL of Hoechst-33342 and incubated for 20–30 min before the cell examination. A Zeiss fluorescent microscope (Carl Zeiss, Jena, Germany), AxioImager A1 camera (at 400 \times magnification), and AxioVision image analysis software Release 4.6.3.0 for Carl Zeiss microscopy (Imaging Associates Ltd., Cork, Ireland, UK) were used for cells examination. All microphotographs were additionally analyzed using ImagePro7 software (Media Cybernetics, Rockville, MD, USA) [65].

3.12. Statistical Data Analysis

The obtained results were analyzed and illustrated with GraphPad Prism (version 8.0.1; GraphPad Software, San Diego, CA, USA). The data were presented as the mean (M) \pm standard deviation (SD), $n = 3-4$. Statistical analyses were performed using two-way ANOVA with Dunnett multiple comparisons test. A p -value of <0.05 was considered statistically significant.

4. Conclusions

This study developed an efficient method for the synthesis of thiopyrano[2,3-*d*]thiazoles containing a naphthoquinone moiety via *hetero*-Diels-Alder reaction using 5-alkyl/arylallylidene-4-thioxo-2-thiazolidinones and 1,4-naphthoquinone. The synthesized compounds were assessed for their antitumor properties according to the DTP NCI protocol. Two synthesized compounds were tested and displayed moderate antitumor activity against leukemia, non-small cell lung cancer, ovarian, breast, prostate cancer, and melanoma cell lines. The 11-phenethyl-3,11-dihydro-2*H*-benzo[6,7]thiochromeno[2,3-*d*]thiazole-2,5,10-trione (3.6) displayed prominent cytotoxicity effects on leukemia (Jurkat, THP-1), epider-

moid (KB3-1, KBC-1), colon (HCT116wt, HCT116 p53-/-), breast (MCF-7), and carcinoma cells. The p53 status of colon carcinoma cells influenced the anti-tumor effects of the studied 3,5,10,11-tetrahydro-2H-benzo[6,7]thiochromeno[2,3-d][1,3]thiazole-2,5,10-trione. We suggest a p53-dependent mode of action for **3.6** towards colon cancer cells. The **3.6** derivative possessed moderate toxicity towards HaCaT, J774.2 cell lines, and isolated normal human lymphocytes. It induced pro-apoptotic cytomorphological changes (chromatin condensation and membrane blabbing) and mitotic catastrophe in treated KB3-1 cells. Compound **3.6** also induced a necrotic death of KB3-1 cells and interacted with DNA. The obtained data revealed the necessity for further investigations among these derivatives in modern anticancer drug therapy.

Supplementary Materials: The following supporting information can be downloaded at: <https://www.mdpi.com/article/10.3390/molecules27217575/s1>, Figures S1–S12: copies of ¹H and ¹³C NMR spectra; Figures S13 and S14: NCI protocols of anticancer activity for compound **3.5** and **3.6**.

Author Contributions: Conceptualization, R.L. and R.S.; methodology, I.I., A.L., J.S., N.F., N.K. and O.K. (Olexandr Karpenko); software, A.G.; validation, O.K. (Olexandr Karpenko), J.S., O.L., A.B., G.S., N.K. and A.L.; formal analysis, N.F. and N.K.; investigation, A.L., I.I., N.F., O.K. (Olga Klyuchivska), N.K., D.L. and A.G.; resources, A.K., S.P., R.S. and R.L.; data curation, N.F. and R.L.; writing—original draft preparation, A.L., I.I., O.L., N.F. and R.L.; writing—review and editing, R.S. and R.L.; visualization, A.L., A.G., I.I. and N.F.; supervision, R.L.; project administration, R.S. and R.L. All authors have read and agreed to the published version of the manuscript.

Funding: The research leading to these results has received funding from the Ministry of Health of Ukraine, under the project number: 0121U100690, and the National Research Foundation of Ukraine, under the project number: 2020.02/0035.

Institutional Review Board Statement: Not applicable.

Informed Consent Statement: The study protocol with human lymphocytes isolated from healthy adult peripheral blood was approved by BioEthics Committee of the Institute of Cell Biology of National Academy of Sciences of Ukraine (protocol No 2 from 27 January 2019), and with written consent of donor.

Data Availability Statement: Not applicable.

Acknowledgments: Authors thank M. Herrmann (Department of Internal Medicine, Institute for Clinical Immunology and Rheumatology, University of Erlangen-Nuremberg, Germany), W. Berger (Institute of Cancer Research, Medical University of Vienna, Austria), John Vane (William Harvey Research Institute, London UK), and Janusz Marcinkiewicz (Jagiellonian University Medical College, Krakow, Poland) for donating cells cultures. The authors would like to thank all the brave defenders of Ukraine who made the finalization of this article possible.

Conflicts of Interest: The authors declare no conflict of interest.

Sample Availability: Samples of compounds **3.1–3.11** are available from the authors.

References

1. Hook, I.; Mills, C.; Sheridan, H. Bioactive naphthoquinones from higher plants. *Stud. Nat. Prod. Chem.* **2014**, *41*, 119–160. [[CrossRef](#)]
2. Medic, A.; Zamljen, T.; Hudina, M.; Solar, A.; Veberic, R. Seasonal variations of naphthoquinone contents (juglone and hydrojuglone glycosides) in *Juglans regia* L. *Sci. Hortic.* **2022**, *300*, 111065. [[CrossRef](#)]
3. Halder, M.; Petsophonsakul, P.; Akbulut, A.C.; Pavlic, A.; Bohan, F.; Anderson, E.; Maresz, K.; Kramann, R.; Schurgers, L. Vitamin K: Double bonds beyond coagulation insights into differences between vitamin K1 and K2 in health and disease. *Int. J. Mol. Sci.* **2019**, *20*, 896. [[CrossRef](#)] [[PubMed](#)]
4. Thijssen, H.H.W.; Vervoort, L.M.T.; Schurgers, L.J.; Shearer, M.J. Menadione is a metabolite of oral vitamin K. *Br. J. Nutr.* **2006**, *95*, 260–266. [[CrossRef](#)] [[PubMed](#)]
5. Comley, J.C.; Sterling, A.M. Effect of atovaquone and atovaquone drug combinations on prophylaxis of *Pneumocystis carinii* pneumonia in SCID mice. *Antimicrob. Agents Chemother.* **1995**, *39*, 806–811. [[CrossRef](#)]
6. Bakshi, R.P.; Tatham, L.M.; Savage, A.C.; Tripathi, A.K.; Mlambo, G.; Ippolito, M.M.; Nenortas, E.; Rannard, S.P.; Owen, A.; Shapiro, T.A. Long-acting injectable atovaquone nanomedicines for malaria prophylaxis. *Nat. Commun.* **2018**, *9*, 315. [[CrossRef](#)]

7. Janeczko, M.; Kubiński, K.; Martyna, A.; Muzyczka, A.; Boguszewska-Czubara, A.; Czernik, S.; Tokarska-Rodak, M.; Chwedczuk, M.; Demchuk, O.M.; Golczyk, H.; et al. 1,4-Naphthoquinone derivatives potently suppress *Candida albicans* growth, inhibit formation of hyphae and show no toxicity toward zebrafish embryos. *J. Med. Microbiol.* **2018**, *67*, 598–609. [[CrossRef](#)]
8. Gopinath, P.; Mahammed, A.; Ohayon, S.; Gross, Z.; Brik, A. Understanding and predicting the potency of ROS-based enzyme inhibitors, exemplified by naphthoquinones and ubiquitin specific protease-2. *Chem. Sci.* **2016**, *7*, 7079–7086. [[CrossRef](#)]
9. Klaus, V.; Hartmann, T.; Gambini, J.; Graf, P.; Stahl, W.; Hartwig, A.; Klotz, L.O. 1,4-Naphthoquinones as inducers of oxidative damage and stress signaling in HaCaT human keratinocytes. *Arch. Biochem. Biophys.* **2010**, *496*, 93–100. [[CrossRef](#)]
10. Pereyra, C.E.; Dantas, R.F.; Ferreira, S.B.; Gomes, L.P.; Silva-Jr, F.P. The diverse mechanisms and anticancer potential of naphthoquinones. *Cancer Cell Int.* **2019**, *19*, 207. [[CrossRef](#)]
11. Tandon, V.K.; Kumar, S. Recent development on naphthoquinone derivatives and their therapeutic applications as anticancer agents. *Expert Opin. Ther. Pat.* **2013**, *23*, 1087–1108. [[CrossRef](#)] [[PubMed](#)]
12. Kretschmer, N.; Rinner, B.; Deutsch, A.J.A.; Lohberger, B.; Knauz, H.; Kunert, O.; Blunder, M.; Boechzelt, H.; Schaidler, H.; Bauer, R. Naphthoquinones from *Onosma paniculata* induce cell-cycle arrest and apoptosis in melanoma cells. *J. Nat. Prod.* **2012**, *75*, 865–869. [[CrossRef](#)] [[PubMed](#)]
13. Kuete, V.; Tangmouo, J.G.; Meyer, J.J.M.; Lall, N. Diospyrone, crassiflorone and plumbagin: Three antimycobacterial and antioncorrhoeal naphthoquinones from two *Diospyros* spp. *Int. J. Antimicrob. Agents* **2009**, *34*, 322–325. [[CrossRef](#)] [[PubMed](#)]
14. Eilenberg, H.; Pnini-Cohen, S.; Rahamim, Y.; Sionov, E.; Segal, E.; Carmeli, S.; Zilberstein, A. Induced production of antifungal naphthoquinones in the pitchers of the carnivorous plant *Nepenthes khasiana*. *J. Exp. Bot.* **2010**, *61*, 911–922. [[CrossRef](#)]
15. Tessele, P.B.; Delle Monache, F.; Quintão, N.L.M.; da Silva, G.F.; Rocha, L.W.; Lucena, G.M.; Ferreira, V.M.M.; Predige, R.D.S.; Cechinel Filho, V. A new naphthoquinone isolated from the bulbs of *Cipura paludosa* and pharmacological activity of two main constituents. *Planta Med.* **2011**, *77*, 1035–1043. [[CrossRef](#)]
16. Milackova, I.; Prnova, M.S.; Majekova, M.; Sotnikova, R.; Stasko, M.; Kovacikova, L.; Banerjee, S.; Veverka, M.; Stefek, M. 2-Chloro-1,4-naphthoquinone derivative of quercetin as an inhibitor of aldose reductase and anti-inflammatory agent. *J. Enzyme Inhib. Med. Chem.* **2015**, *30*, 107–113. [[CrossRef](#)]
17. Onegi, B.; Kraft, C.; Köhler, I.; Freund, M.; Jenett-Siems, K.; Siems, K.; Beyer, G.; Melzig, M.F.; Bienzle, U.; Eich, E. Antiplasmodial activity of naphthoquinones and one anthraquinone from *Stereospermum kunthianum*. *Phytochemistry* **2002**, *60*, 39–44. [[CrossRef](#)]
18. Fotie, J. Quinones and malaria. *Antiinfect. Agents Med. Chem.* **2006**, *5*, 357–366. [[CrossRef](#)]
19. González, A.; Becerra, N.; Kashif, M.; González, M.; Cerecetto, H.; Aguilera, E.; Nogueira-Torres, B.; Chacón-Vargas, K.F.; Zarate-Ramos, J.J.; Castillo-Velázquez, U.; et al. In vitro and in silico evaluations of new aryloxy-1,4-naphthoquinones as anti-*Trypanosoma cruzi* agents. *Med. Chem. Res.* **2020**, *29*, 665–674. [[CrossRef](#)]
20. Ventura Pinto, A.; Lisboa de Castro, S. The trypanocidal activity of naphthoquinones: A review. *Molecules* **2009**, *14*, 4570–4590. [[CrossRef](#)]
21. Lawrence, H.R.; Kazi, A.; Luo, Y.; Kendig, R.; Ge, Y.; Jain, S.; Daniel, K.; Santiago, D.; Guida, W.C.; Sebt, S.M. Synthesis and biological evaluation of naphthoquinone analogs as a novel class of proteasome inhibitors. *Bioorg. Med. Chem.* **2010**, *18*, 5576–5592. [[CrossRef](#)] [[PubMed](#)]
22. Kar, S.; Wang, M.; Ham, S.W.; Carr, B.I. Fluorinated Cpd 5, a pure arylating K-vitamin derivative, inhibits human hepatoma cell growth by inhibiting Cdc25 and activating MAPK. *Biochem. Pharmacol.* **2006**, *72*, 1217–1227. [[CrossRef](#)] [[PubMed](#)]
23. Krishnan, P.; Bastow, K.F. Novel mechanisms of DNA topoisomerase II inhibition by pyranonaphthoquinone derivatives—Eleutherin, α lapachone, and β lapachone*. *Biochem. Pharmacol.* **2000**, *60*, 1367–1379. [[CrossRef](#)]
24. Chae, G.H.; Song, G.Y.; Kim, Y.; Cho, H.; Sok, D.E.; Ahn, B.Z. 2-or 6-(1-azidoalkyl)-5,8-dimethoxy-1,4-naphthoquinone: Synthesis, evaluation of cytotoxic activity; antitumor activity and inhibitory effect on DNA topoisomerase-I. *Arch. Pharm. Res.* **1999**, *22*, 507–514. [[CrossRef](#)] [[PubMed](#)]
25. Godoy-Castillo, C.; Bravo-Acuña, N.; Arriagada, G.; Faunes, F.; León, R.; Soto-Delgado, J. Identification of the naphthoquinone derivative inhibitors binding site in heat shock protein 90: An induced-fit docking, molecular dynamics and 3D-QSAR study. *J. Biomol. Struct. Dyn.* **2021**, *39*, 5977–5987. [[CrossRef](#)] [[PubMed](#)]
26. Karkare, S.; Chung, T.T.H.; Collin, F.; Mitchenall, L.A.; McKay, A.R.; Greive, S.J.; Meyer, J.J.M.; Lall, N.; Maxwell, A. The naphthoquinone diospyrin is an inhibitor of DNA gyrase with a novel mechanism of action. *J. Biol. Chem.* **2013**, *288*, 5149–5156. [[CrossRef](#)]
27. Kim, T.J.; Yun, Y.P. Antiproliferative activity of NQ304, a synthetic 1,4-naphthoquinone, is mediated via the suppressions of the PI3K/Akt and ERK1/2 signaling pathways in PDGF-BB-stimulated vascular smooth muscle cells. *Vascul. Pharmacol.* **2007**, *46*, 43–51. [[CrossRef](#)]
28. Song, H.; Wang, R.; Wang, S.; Lin, J. A low-molecular-weight compound discovered through virtual database screening inhibits Stat3 function in breast cancer cells. *Proc. Natl. Acad. Sci. USA.* **2005**, *102*, 4700–4705. [[CrossRef](#)]
29. Komiyama, T.; Takaguchi, Y.; Tsuboi, S. Synthesis of anthraquinone derivatives: Tandem Diels-Alder-decarboxylation-oxidation reaction of 3-hydroxy-2-pyrone with 1,4-naphthoquinone. *Synlett* **2006**, *1*, 0124–0126. [[CrossRef](#)]
30. Carreño, M.C.; García-Cerrada, S.; Urbano, A.; Di Vitta, C. Studies of Diastereoselectivity in Diels-Alder Reactions of Enantiopure (SS)-2-(*p*-Tolylsulfinyl)-1, 4-naphthoquinone and Chiral Racemic Acyclic Dienes. *J. Org. Chem.* **2000**, *65*, 4355–4363. [[CrossRef](#)]

31. Carreño, M.C.; Urbano, A.; Di Vitta, C. Enantioselective Diels–Alder Cycloadditions with (SS)-2-(p-Tolylsulfinyl)-1,4-naphthoquinone: Efficient Kinetic Resolution of Chiral Racemic Vinylcyclohexenes. *J. Org. Chem.* **1998**, *63*, 8320–8330. [[CrossRef](#)]
32. Brimble, M.A.; McEwan, J.F. Use of bis(oxazoline)-metal complexes as chiral catalysts for asymmetric Diels–Alder reactions using 2-acetyl-1,4-naphthoquinone as a dienophile. *Tetrahedron Asymmetry* **1997**, *8*, 4069–4078. [[CrossRef](#)]
33. Carreño, M.C.; Urbano, A.; Di Vitta, C. Enantioselective Diels–Alder Approach to C-3-Oxygenated Angucyclinones from (SS)-2-(p-Tolylsulfinyl)-1,4-naphthoquinone. *Chem. Eur. J.* **2000**, *6*, 906–913. [[CrossRef](#)]
34. Khatri, A.I.; Samant, S.D. Facile, Diversity-Oriented, Normal-Electron-Demand Diels–Alder Reactions of 6-Amino-2H-pyran-2-ones with Diethyl Acetylenedicarboxylate, 1,4-Naphthoquinone, and N-Phenylmaleimide. *Synthesis* **2015**, *47*, 343–350. [[CrossRef](#)]
35. Landells, J.S.; Larsen, D.S.; Simpson, J. Remote stereochemical control in asymmetric Diels–Alder reactions: Synthesis of the angucycline antibiotics, (–)-tetrangomycin and MM 47755. *Tetrahedron Lett.* **2003**, *44*, 5193–5196. [[CrossRef](#)]
36. Kryshchshyn, A.; Atamanyuk, D.; Lesyk, R. Fused thiopyrano[2,3-d]thiazole derivatives as potential anticancer agents. *Sci. Pharm.* **2012**, *80*, 509–530. [[CrossRef](#)]
37. Metwally, N.H.; Badawy, M.A.; Okpy, D.S. Synthesis and anticancer activity of some new thiopyrano[2,3-d]thiazoles incorporating pyrazole moiety. *Chem. Pharm. Bull.* **2015**, *63*, 495–503. [[CrossRef](#)]
38. Atamanyuk, D.; Zimenkovsky, B.; Atamanyuk, V.; Nektgayev, I.; Lesyk, R. Synthesis and biological activity of new thiopyrano[2,3-d]thiazoles containing a naphthoquinone moiety. *Sci. Pharm.* **2013**, *81*, 423–436. [[CrossRef](#)]
39. Lozynskiy, A.; Zasadko, V.; Atamanyuk, D.; Kaminsky, D.; Derkach, H.; Karpenko, O.; Ogurtsov, V.; Kutsyk, R.; Lesyk, R. Synthesis, antioxidant and antimicrobial activities of novel thiopyrano[2,3-d]thiazoles based on acryloyl acids. *Mol. Divers.* **2017**, *21*, 427–436. [[CrossRef](#)]
40. Zelisko, N.; Atamanyuk, D.; Vasylenko, O.; Grellier, P.; Lesyk, R. Synthesis and antitrypanosomal activity of new 6, 6, 7-trisubstituted thiopyrano[2,3-d][1,3]thiazoles. *Bioorg. Med. Chem. Lett.* **2012**, *22*, 7071–7074. [[CrossRef](#)]
41. Lozynskiy, A.; Zimenkovsky, B.; Nektgayev, I.; Lesyk, R. Arylidene pyruvic acids motif in the synthesis of new thiopyrano[2,3-d]thiazoles as potential biologically active compounds. *Heterocycl. Commun.* **2015**, *21*, 55–59. [[CrossRef](#)]
42. Lozynskiy, A.; Karkhut, A.; Polovkovych, S.; Karpenko, O.; Holota, S.; Gzella, A.K.; Lesyk, R. 3-Phenylpropanal and citral in the multicomponent synthesis of novel thiopyrano[2,3-d]thiazoles. *Results Chem.* **2022**, *4*, 100464. [[CrossRef](#)]
43. Allen, F.H.; Kennard, O.; Watson, D.G.; Brammer, L.; Orpen, A.G.; Taylor, R. Tables of bond lengths determined by X-ray and neutron diffraction. Part 1. Bond lengths in organic compounds. *J. Chem. Soc. Perkin Trans. 2* **1987**, S1–S19. [[CrossRef](#)]
44. Boyd, M.R.; Paull, K.D. Some practical considerations and applications of the National Cancer Institute in vitro anticancer drug discovery screen. *Drug Dev. Res.* **1995**, *34*, 91–109. [[CrossRef](#)]
45. Shoemaker, R.H. The NCI60 human tumour cell line anticancer drug screen. *Nat. Rev. Cancer* **2006**, *6*, 813–823. [[CrossRef](#)]
46. Monks, A.; Scudiero, D.; Skehan, P.; Shoemaker, R.; Paull, K.; Vistica, D.; Hose, C.; Langley, J.; Cronise, P.; Boyd, M.; et al. Feasibility of a high-flux anticancer drug screen using a diverse panel of cultured human tumor cell lines. *J. Natl. Cancer Inst.* **1991**, *83*, 757–766. [[CrossRef](#)]
47. Tedesco, S.; De Majo, F.; Kim, J.; Trenti, A.; Trevisi, L.; Fadini, G.P.; Bolego, C.; Zandstra, P.W.; Cignarella, A.; Vitiello, L. Convenience versus biological significance: Are PMA-differentiated THP-1 cells a reliable substitute for blood-derived macrophages when studying in vitro polarization? *Front. Pharmacol.* **2018**, *9*, 71. [[CrossRef](#)]
48. Podolski-Renić, A.; Dinić, J.; Stanković, T.; Tsakovska, I.; Pajeva, I.; Tuccinardi, T.; Botta, L.; Schenone, S.; Pešić, M. New Therapeutic Strategy for Overcoming Multidrug Resistance in Cancer Cells with Pyrazolo[3,4-d]pyrimidine Tyrosine Kinase Inhibitors. *Cancers* **2021**, *13*, 5308. [[CrossRef](#)]
49. Dabiri, Y.; Abu el Maaty, M.A.; Chan, H.Y.; Wölker, J.; Ott, I.; Wölfl, S.; Cheng, X. p53-dependent anti-proliferative and pro-apoptotic effects of a gold (I) N-heterocyclic carbene (NHC) complex in colorectal cancer cells. *Front. Oncol.* **2019**, *9*, 438. [[CrossRef](#)]
50. Theodossiou, T.A.; Ali, M.; Grigalavicius, M.; Grallert, B.; Dillard, P.; Schink, K.O.; Olsen, C.E.; Wälchli, S.; Inderberg, E.M.; Kubin, A.; et al. Simultaneous defeat of MCF7 and MDA-MB-231 resistances by a hypericin PDT–tamoxifen hybrid therapy. *NPJ Breast Cancer* **2019**, *5*, 13. [[CrossRef](#)]
51. Vakifahmetoglu, H.; Olsson, M.; Zhivotovsky, B. Death through a tragedy: Mitotic catastrophe. *Cell Death Differ.* **2008**, *15*, 1153–1162. [[CrossRef](#)] [[PubMed](#)]
52. Garas, A.; Webb, E.; Pillay, V.; MacPhee, D.; Denny, W.; Zeller, H.; Cotton, R. A novel and simple method of screening compounds for interaction with DNA: A validation study. *Mutat. Res. Genet. Toxicol. Environ. Mutagen.* **2009**, *678*, 20–29. [[CrossRef](#)] [[PubMed](#)]
53. Kim, S.K.; Nordén, B. Methyl green: A DNA major-groove binding drug. *FEBS Lett.* **1993**, *315*, 61–64. [[CrossRef](#)]
54. Elsayed, S.A.; Saad, E.A.; Mostafa, S.I. Development of new potential anticancer metal complexes derived from 2-hydrazinobenzothiazole. *Mini-Rev. Med. Chem.* **2019**, *19*, 913–922. [[CrossRef](#)]
55. Kaminsky, D.; Vasylenko, O.; Atamanyuk, D.; Gzella, A.; Lesyk, R. Isorhodanine and thiorhodanine motifs in the synthesis of fused thiopyrano[2,3-d][1,3]thiazoles. *Synlett* **2011**, *10*, 1385–1388. [[CrossRef](#)]
56. Rigaku Oxford Diffraction. *CrysAlis PRO, Version 1.171.40.67a*; Rigaku Oxford Diffraction: Yarnton, UK, 2019.
57. Sheldrick, G. SHELXT—Integrated space-group and crystal-structure determination. *Acta Crystallogr. Sect. A* **2015**, *71*, 3–8. [[CrossRef](#)]
58. Sheldrick, G. Crystal structure refinement with SHELXL. *Acta Crystallogr. Sect. C* **2015**, *71*, 3–8. [[CrossRef](#)]

59. Dolomanov, O.V.; Bourhis, L.J.; Gildea, R.J.; Howard, J.A.K.; Puschmann, H. OLEX2: A complete structure solution, refinement and analysis program. *J. Appl. Crystallogr.* **2009**, *42*, 339–341. [[CrossRef](#)]
60. Farrugia, L.J. WinGX and ORTEP for Windows: An update. *J. Appl. Crystallogr.* **2012**, *45*, 849–854. [[CrossRef](#)]
61. Spek, A. Structure validation in chemical crystallography. *Acta Crystallogr. Sect. D* **2009**, *65*, 148–155. [[CrossRef](#)]
62. Alisik, M.; Neselioglu, S.; Erel, O. A colorimetric method to measure oxidized, reduced and total glutathione levels in erythrocytes. *J. Lab. Med.* **2019**, *43*, 269–277. [[CrossRef](#)]
63. Finiuk, N.; Kryshchshyn-Dylevych, A.; Holota, S.; Klyuchivska, O.; Kozytskiy, A.; Karpenko, O.; Manko, N.; Ivasechko, I.; Stoika, R.; Lesyk, R. Novel hybrid pyrrolidinedione-thiazolidinones as potential anticancer agents: Synthesis and biological evaluation. *Eur. J. Med. Chem.* **2022**, *238*, 114422. [[CrossRef](#)] [[PubMed](#)]
64. Herrmann, M.; Lorenz, H.M.; Voll, R.E.; Grünke, M.; Woith, W.; Kalden, J.R. A rapid and simple method for the isolation of apoptotic DNA fragments. *Nucleic Acids Res.* **1994**, *22*, 5506–5507. [[CrossRef](#)] [[PubMed](#)]
65. Finiuk, N.; Klyuchivska, O.; Ivasechko, I.; Hreniukh, V.; Ostapiuk, Y.; Shalai, Y.; Panchuk, R.; Matiychuk, V.; Obushak, M.; Stoika, R.; et al. Proapoptotic effects of novel thiazole derivative on human glioma cells. *Anti-Cancer Drugs* **2019**, *30*, 27–37. [[CrossRef](#)] [[PubMed](#)]